ChemPubSoc Europe

DOI: 10.1002/chem.201402694

CHEMISTRY
A European Journal
Full Paper

Magnetic Anisotropy

Magnetic Anisotropy of Mononuclear Ni^{II} Complexes: On the Importance of Structural Diversity and the Structural Distortions

Saurabh Kumar Singh, Tulika Gupta, Prashi Badkur, and Gopalan Rajaraman*[a]

Abstract: Mononuclear Ni^{II} complexes are particularly attractive in the area of single-molecule magnets as the axial zero-field splitting (D) for the Ni^{II} complexes is in the range of -200 to $+200\ cm^{-1}$. Despite this advantage, very little is known on the origin of anisotropy across various coordination ligands, coordination numbers, and particularly what factors influence the D parameter in these complexes. To answer some of these questions, herein we have undertaken a detailed study of a series of mononuclear Ni^{II} complexes with ab initio calculations. Our results demonstrate that three prominent spin-conserved low-lying d–d transitions contribute significantly to the D value. Variation in the sign and the magnitude of D values are found to correlate to the specific structural distortions. Apart from the metal–ligand bond lengths, two different parameters, namely, $\Delta\alpha$ and $\Delta\beta$, which are correlated to the *cis* angles present in the coordination environment, are found to significantly influence the axial D values. Developed magneto–structural D correlations suggest that the D values can be enhanced significantly by fine tuning the structural distortion in the coordination environment. Calculations performed on a series of Ni^{II} models with coordination numbers two to six unfold an interesting observation—the D parameter increases significantly upon a reduction in coordination number compared with a reference octahedral coordination. Besides, if high symmetry is maintained, even larger coordination numbers yield large D values.

Introduction

In recent years single-molecule magnets (SMMs)[1] have emerged as promising materials for information-storage devices[1] along with other potential applications, such as molecular coolants[2] and quantum computing.[3] These SMMs exhibit slow relaxation of magnetization below the blocking temperature in the absence of a magnetic field. This occurs due to an energy barrier between the spin microstates, the so-called ms levels. This energy barrier (U_{eff}) is given by $|D|S^2$ (for integer spin states), but is found to be largely independent of the total spin (S) as D is inversely proportional to S^2.[4] Moreover, for half-integer spin ground state, even positive D values are found to exhibit SMM behavior.[5] Large polynuclear clusters often yield large S, but negligible D values,[6] whereas the mononuclear complexes often possess large magnetic anisotropy.[7–8] Hence, with the hope of designing SMMs with large negative D values from the promising mononuclear complexes, numerous mononuclear transition-metal complexes have been synthesized lately, and, indeed, many of them were found to possess larger U_{eff} values than traditional polynuclear transition-metal clusters.[7–9] Because only a finite S value, depending on the number of unpaired electrons, can be obtained in mononuclear complexes, fine tuning the magnetic properties of these system largely rely on the zero-field splitting parameter, thus understanding and controlling the zero-field splitting (zfs) parameter is of paramount importance. In this regard, mononuclear Fe^{II}, Co^{II}, and Ni^{II} complexes[9b,10–13] have attracted the interest of the magnetism community as some of these complexes are reported to have impressive zfs values, as large as approximately $-200\ cm^{-1}$, and large U_{eff} values. These are commonly called single-ion magnets (SIMs) and in the last few years several SIMs that possess unusual coordination numbers (CNs) have been reported and some of these complexes yield U_{eff} values as large as $226\ cm^{-1}$.[9b] Besides transition metals, lanthanides based SIMs have been of great interest in recent years because they inherit large magnetic anisotropy.[7a,14] An illustrating example is the mononuclear $[Er(COT)_2]^-$ (COT = cyclooctatetraene) complex[15] that possesses a record blocking temperature (T_B) of 10 K required for magnetization reversal.

Most of the reported transition-metal-based SMMs possess Mn^{III} ions, because they generally offer negative D values due to common Jahn–Teller elongated structures. Extensive experimental and theoretical studies reveal that the D parameters in six-coordinated Mn^{III} complexes are, however, small and in the range of -5 to $+5\ cm^{-1}$.[16] Theoretical studies to underpin the origin of zfs in Mn^{III} have thus been undertaken; these studies highlight the role of the spin–spin part in estimating the zfs parameters.[16a,17] On similar lines, the origin of the zfs parameter in Fe^{II} complexes with out-of-state spin–orbit coupling has

[a] S. K. Singh, T. Gupta, P. Badkur, Prof. Dr. G. Rajaraman
Department of Chemistry
Indian Institute of Technology Bombay
Powai,Mumbai,Maharashtra,India-400 076
Fax: (+91) 22-2576-7152
E-mail: rajaraman@chem.iitb.ac.in

Supporting information for this article is available on the WWW under http://dx.doi.org/10.1002/chem.201402694.

also been explored.[18] The dependence of the zfs parameter on the basicity of the donor ligands for some mononuclear Fe^{II} and Co^{II} complexes have also been demonstrated.[18]

Although Mn^{III}, Fe^{II}, and Co^{II} ions are commonly employed among the first row transition-metal ions to obtain SMMs, Ni^{II} ions also successfully yield SMMs with attractive barrier heights.[18a,19] The first Ni^{II}-ion-based SMM was prepared by Winpenny and co-workers, who synthesized a giant $\{Ni_{12}\}$ wheel possessing an $S=12$ ground state and $D=-0.047\ cm^{-1}$. This molecule is reported to have U_{eff} of 9.6 K.[19a] Following by this discovery, several other Ni^{II}-based SMMs have been reported, including some mononuclear complexes.[19] Neese and co-workers[20] and Maurice and co-workers[9a,21] independently, by the use of theoretical tools, probed the origin of zfs in a series of mononuclear Ni^{II} complexes and significant insight into the role of halide ions as well as the coordination sphere in determining the magnitude of the zfs parameter was established. On the other hand, Comba and co-workers studied spectroscopic and magnetic data of a series of Ni^{II} bispidine complexes and probed the anisotropy of these complexes by the use of an angular overlap model and ab initio calculations.[20a,22–23] These studies have recently been extended to dinuclear Ni^{II} complexes.[24]

Experimentally probing the microscopic origin of the zfs parameter is often challenging and has been attempted only in a few selected cases by using multifrequency EPR and other techniques.[25] On the other hand, theoretical studies play a prominent role in probing the microscopic origin of zfs parameters. Despite the increased number of Ni^{II}-based SMMs since the first report,[19a] the electronic or structural origin of zfs in various types of Ni^{II} complexes still remain unexplored.[9a,26,27] Based on ligand-field theory, Abragam and Bleaney proposed the following qualitative equation [Eq (1)] for the D values in Ni^{II} complexes, in which λ = spin–orbit coupling constant Δ = crystal field splitting parameter:

$$D = -\frac{4\lambda^2}{\Delta_1} + \frac{4\lambda^2}{\Delta_2} \qquad (1)$$

As per Equation (1), if a compression is applied on the z axis $\Delta_1 < \Delta_2$, hence D is negative, whereas elongation leads to $\Delta_1 > \Delta_2$ and a positive D value.[23] In an effort towards understanding the same, a series of Ni^{II} mononuclear complexes were reported and their zfs values were estimated based on fitting of powder susceptibility and magnetization data.[28–29] Based on the available data, a correlation to zfs values has been proposed based on the tetragonality parameter D_{str} of the complexes. To offer a clear-cut understanding of zfs in varied coordination environments and to ascertain the factors on which the sign and magnitude of this parameter depend, herein we have undertaken detailed ab initio calculations of zfs parameters in a series of mononuclear Ni^{II} complexes. We have also developed magneto–structural D correlations to offer clues on how to enhance the zfs further in a given coordination environment for a Ni^{II} complexes.[26]

Computational Details

Calculations were performed by using the ORCA program[30] package for eleven complexes for which the X-ray structures[31] as well as zfs parameters are available from experiments. There are two contributions to the zfs parameter, the first and the prominent one being the spin–orbit coupling (SOC) contribution and the second being the dipolar spin–spin (SS) contribution to the D value.[16a,17,32] Although the density functional calculations are widely used for the estimation of zfs parameters for polynuclear complexes,[33] generally the computed zfs parameters are less accurate compared with ab initio treatment.[1c,20,26]

The ab initio CASSCF calculations were performed by using the ORCA suite of programs and here we have performed the state-average complete active space self-consistent field (SA-CASSCF) calculations incorporating the required excited states. We employed the def2-TZVPP basis set for Ni and def2-TZVP for the rest of the atoms during the zfs calculations.[34] The SA-CASSCF calculations have a history of yielding accurate estimation of D and E parameters for transition-metal complexes (where D signifies axial zfs and E describes rhombic zfs).[16a,17–18,20–21] The active space for CASSCF calculations comprises five Ni^{II}-based orbitals with eight electrons in them (d^8 system; CAS(8,5) setup). We considered ten triplet excited states and fifteen singlet excited states in our calculations to compute zfs in these 11 complexes.[17a] The SOC contributions in the ab initio frame work were obtained by using the second-order perturbation theory (2PT; Table 1) as well as employing the effective Hamiltonian approach (EHA; Table S5 in the Supporting Information), which enables calculations of all matrix elements of the anisotropic spin Hamiltonian from the ab initio energies and wave functions numerically.[35] To treat the dynamic correlations, N-electron valence perturbation theory (NEVPT2) calculations[36] on SA-CASSCF (non-dynamic electron correlation) converged wave functions were performed. The CASSCF wave function contains all electronic configurations that can be constructed by distributing eight electrons over the five 3d orbitals of the Ni^{II} ions. The SS coupling contribution was estimated from the SS coupling operator by using the mean-field approximation.[35] In light of the recent discussion[16a,17,20] and considering the superiority of the NEVPT2 correlated energies towards the estimation of zfs parameters, here we restricted our analysis to NEVPT2-2PT results, unless otherwise mentioned.

Additional ab initio calculations were also performed by using the MOLCAS 7.8[37] suite on model systems in which orbital degeneracy are expected. Here we employed the [ANO-RCC.. 6s5p3d2f1g.] basis set for Ni, the [ANO-RCC.. 3 s2p1d.] basis set for N, and the [ANO-RCC.. 2s.] basis set for H atoms. First we performed CASSCF calculations with an active space of eight active electrons in five 3d orbitals (8,5). With this active space, we computed 10 triplets as well as 15 singlets in the configuration interaction (CI) procedure. After computing these excited states, we mixed all these 10 triplets and 15 singlets by using the RASSI-SO[38] module to compute the SOC states. Due to hardware limitations we did not performed second-order CASPT2 calculations here. Further on, we took these computed SO states into the SINGLE ANISO[37b] program to compute the D-tensors. The Cholesky decomposition for two electron integrals was employed throughout.

Results and Discussion

Boca and co-workers reported zfs values of a series of Ni^{II} mononuclear complexes with structures varying from compressed tetragonal systems to elongated ones. These were classified

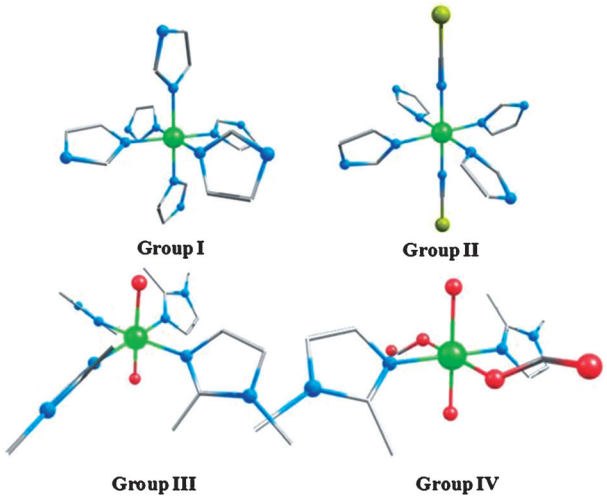

Figure 1. Four crystal structures as representatives for Groups I–IV are shown. The hydrogens atoms are omitted for the clarity. Color code: Ni green, O red, N blue, S yellow, C gray.

Table 1. List of complexes studied along with experimental and computed zfs parameters.

Complex[a]	D_{exp} [cm^{-1}]	NEVPT2-2PT-calculated D/E values		
		D_{cal} [cm^{-1}]	E_{cal}/D_{cal}	g_{cal}
Group I				
a) $[Ni(iz)_6](fm)_2$	−3.43	−3.66	0.25	2.4668
b) $[Ni(iz)_6](Cl\text{-}ac)_2$	≈0	−0.56	0.17	2.4196
c) $[Ni(iz)_6](Cl\text{-}prop)_2$	0.9	−1.44	0.17	2.4227
Group II				
a) $[Ni(iqu)_4(NCS)_2]$	−1.54	1.02	0.26	2.4268
b) $[Ni(Mefpy)_4(NCS)_2]$	−1.93	5.11	0.01	2.4621
Group III				
a) $[Ni(pz)_4(ac)_2]$	3.88	4.09	0.09	2.4492
b) $[Ni(dmeiz)_4(H_2O)_2]Cl_2$	7.42	10.67	0.10	2.4978
Group IV				
a) $[Ni(dmeiz)_2(fm)_2(H_2O_2]$	−7.7	8.79	0.30	2.5777
b) $[Ni(fpy)_2(ac)_2(H_2O)_2]$	−5	3.99	0.14	2.4912
c) $[Ni(iqu)_2(ac)_2(H_2O)_2]$	−5.3	5.58	0.32	2.5271
d) $[Ni(bzfpy)_2(ac)_2(H_2O)_2]$	−2.85	4.93	0.18	2.5027

[a] iz = imidazole, fm = formato, iqu = isoquinoline, Mefpy = 2-methylfuro-[3,2-*c*]pyridine, pz = pyrazole, demiz = 1,2-dimethyl-imidazole, fpy = furo[3,2-*c*]pyridine, bzfpy = benzo[4,5]furo[3,2-c]pyridine.

into four categories: Group I (homoleptic complexes), Group II (quasi-octahedral), Group III (tetragonal), and Group IV (rhombic systems; see Figure 1) based on the coordination atom types and the structures. Each of these complexes was characterized by a tetragonality parameter, D_{str}, to which the fitted magnetic D value, D_{mag}, was correlated. The D_{str} of the first group was defined differently than the other three as they are the only homoleptic complexes in the set. Equation (2) was advocated to evaluate D_{str} for Group I ({NiN_6}) complexes

$$D_{str} = R_{ax} - R_{eq}\ cm^{-1} \quad (2)$$

where R_{ax} refers to the axial bond length and R_{eq} refers to the average equatorial bond length. A different formula was used for the remaining three groups {NiN_4N_2'} (Group II), {NiN_4O_2} (Group III), and {$NiN_2O_2O_2'$} (Group IV), details of which are discussed elsewhere (see the Supporting Information, Table S1 for details).[28,29] In order to shed light on how the zfs parameter varies across these groups and to probe the effect of metal–ligand bond strength as well as the covalency on the estimated D values, CASSCF calculations were performed (see Table 1). Although the magnitude of D is reproduced compared with the experimental estimate across all the groups, the sign of D is contrary to the experimental values for Group II and IV. 2PT and the EHA yield similar signs and magnitudes of D across the series computed (see the Supporting Information, Table S5) and this adds confidence to the computed results. To obtain further clues on the sign of the D values,[16b] we performed additional simulations with the Phi program where both the magnetization and the susceptibility data were simultaneously employed to fit the data (see the Supporting Information for descriptive details on the usage of the Phi program).[39] Although this resolve the sign ambiguity in two cases, both positive and negative D fits the experimental data equally well for other complexes and two distinct minima are clearly found in a residual error plot. The computed D values also yield good fits to the experimental magnetization and susceptibility data (Figure S2–S23 in the Supporting Information). Because accurate measurements, such as HF-EPR spectroscopic data, are not available for these complexes, the issue related to the sign of the D values cannot be resolved by experimental means.

Studies on Group I: {NiN_6} homoleptic complexes

In the first group, three complexes were chosen and all these structures have the common formula of $[Ni(iz)_6]^{2+}$, however there are some structural deviations within the compounds that are associated to the different counter anions (see Table 1). This class is ideal to make the comparison as all the ligands are identical and any difference in the D parameter must be associated to the small structural distortion directed by the counter anion. As D_{str} is related to the difference in the axial and equatorial bond lengths, a perfect octahedral structure would yield a D value of zero, consistent with the symmetry arguments.[40] Even a slight distortion from the perfect octahedral symmetry is enough to yield a non-zero D value. The computed trend correlates with the experiments, although a deviation in sign is evident for complex Ic.

Studies on Group II: {$NiN_4N'_2$} complexes

The complexes of this group comprise a slightly diverse coordination sphere with the axial positions occupied by the thiocyanato ligands and the equatorial plane coordinate by a quinoline/furopyridine-based N-donor ligand. Although the magnitude of D is reproduced in our calculations, the sign of D is contrary to the experiment. Complex IIa and IIb are structurally similar, but possess different D values due to disparity in the basicity of the N-donor ligands in the equatorial plane (isoquinoline in case of complex IIa and Mefpy in case of IIb). The

computed *D* values for both complexes are found to be positive. Analyzing different contributions to *D* suggests that the major contribution that adds to the negative part of *D* arises from excitation I (see the Supporting Information for details) and this excitation is similar to that of the complexes studied in Group I with a major contributory transition being $d_{yz} \rightarrow d_{z^2}$ (dark green line in Figure 2 and complex IIb in Figure 3). The contribution due to this excitation is the same in both cases as the axial ligands are the same with almost similar α-*cis*-angle (see Table 2 and Table S2 in the Supporting Information).

Here the difference in the magnitude of *D* arise from excitations II and III (these are predominantly $d_{xz} \rightarrow d_{x^2-y^2}$ and $d_{xy} \rightarrow d_{x^2-y^2}$ transitions). The energies of these orbitals are found to correlate to the equatorial angles defined as the $\Delta\beta$ parameter in Scheme 1.

Table 2. List of key excitation energies arising from the low-lying d–d multiplets observed for the studied complexes along with the contribution to the *D* values.

Complex	Excitation I		Excitation II		Excitation III	
	Energy [cm^{-1}]	*D* [cm^{-1}]	Energy [cm^{-1}]	*D* [cm^{-1}]	Energy [cm^{-1}]	*D* [cm^{-1}]
Group I						
Ia	10935	−38.7	11739	17.6	12210	17.1
Ib	11961	−34.6	12123	17.3	12074	16.8
Ic	11941	−35.7	12241	17.3	12529	16.5
Group II						
IIa	12120	−33.1	11823	17	11790	16.8
IIb	12560	−33.5	10855	19.8	10818	19.1
Group III						
IIIa	10255	−36.2	10422	20.6	10438	20.6
IIIb	13230	−32.8	9062	23.2	8906	23.8
Group IV						
IVa	8555	−37.2	11501	22	9581	25.1
IVb	9077	−41.8	10107	24.1	9077	23.4
IVc	9490	−36.5	11437	20.3	10378	22.8
IVd	10069	−36.7	11358	21.8	10451	20.5

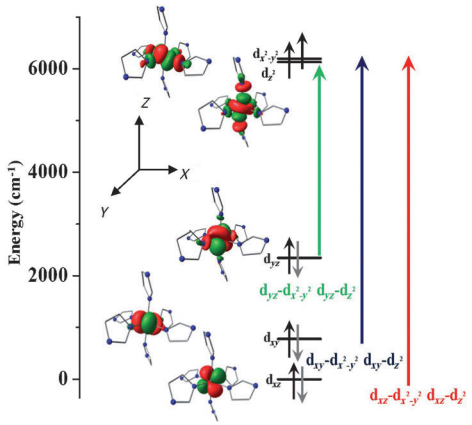

Figure 2. CASSCF-computed metal-based d orbitals with single excitations. The picture shows all possible spin-conserved excitations responsible for the zfs for the set tested (the orbitals and the energies is for complex Ib). The green and red regions indicate positive and negative spin phases. The isodensity surface represented corresponds to a value of $0.015e^{-}$ $bohr^{-3}$.

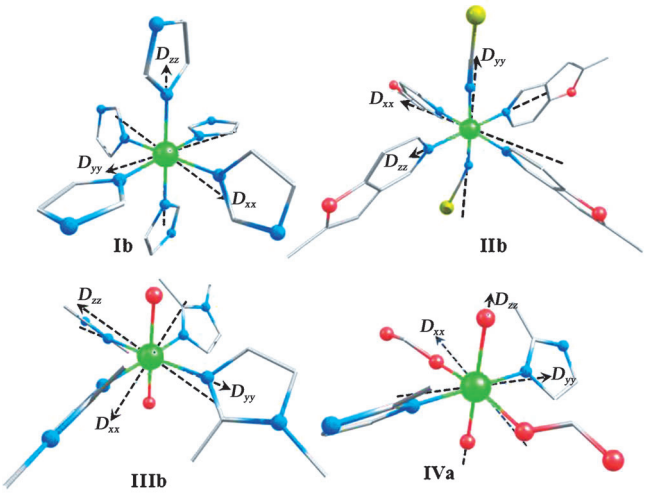

Figure 3. NEVPT2-computed orientation of the zfs tensors for complexes Ib, IIb, IIIb, and IVa as representatives for each group. See Figure S1 in the Supporting Information for details. The color code is same as in the Figure 1.

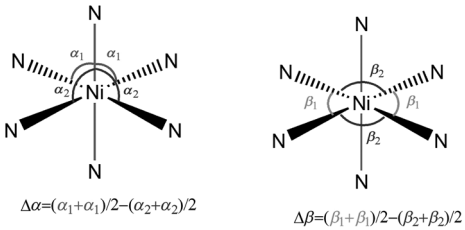

Scheme 1. Schematic illustration of the $\Delta\alpha$ and $\Delta\beta$ parameters present in these complexes.

This parameter is estimated to 0.7 and 6.0 for IIa and IIb, respectively. This difference significantly affects the energies of d_{xy} and $d_{x^2-y^2}$ orbitals. For an ideal octahedral geometry, the $\Delta\beta$ parameter is zero (see Scheme 1) and a large value of $\Delta\beta$ suggests a significant structural distortion from ideal symmetry. As the $\Delta\beta$ value increases, the σ-donor ligand orbitals start to interact with the t_{2g} orbitals and this leads to destabilization of these orbitals (see Figure 4). Here the $N(p_x)$ orbital of the ligand is found to interact with $Ni(d_{xy})$ orbital as the $\Delta\beta$ increases and this in turn raises the energy of the d_{xy} orbital. A large $\Delta\beta$ also means that the ligand deviates from the axial direction and thus the interaction with the $Ni(d_{x^2-y^2})$ weakens; this stabilizes this orbital, leading to a drastic reduction in the $d_{xz} \rightarrow d_{x^2-y^2}$ and $d_{xy} \rightarrow d_{x^2-y^2}$ gaps (see Figure 4). This reduction observed for IIb rationalizes the observed deviation in the computed *D* values. We would like to note here that at some instance this parameter may not reflect the distortion present in a structure, thus one has to carefully also inspect the individual *cis* angles (see Table S2 in the Supporting Information).

Studies on Group III: $\{NiN_4O_2\}$ complexes

Group III complexes are structurally diverse with the axial positions occupied by O-donor ligands and the equatorial positions by the N-donor ligands. Here two representative complexes, namely, IIIa and IIIb, are studied where the axial position is occupied by acetate and water molecules, respectively (see

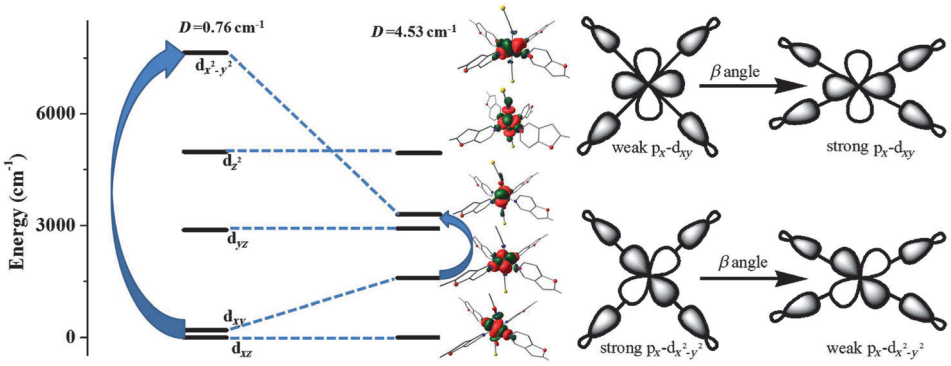

Figure 4. CASSCF-computed Eigen value plot along with metal-based orbitals for complexes IIa and IIb (left). The blue arrows correspond to the dominant ($d_{xy} \rightarrow d_{x^2-y^2}$) excitation, which is responsible for alteration of the *D* values. The orbital interaction diagram reflects the extent of interaction as the $\Delta\beta$ parameter varies (right). The green and red regions indicate positive and negative spin phases. The isodensity surface represented corresponds to a value of 0.015e$^-$ bohr^{-3}.

Figure 1 and Figure S1 in the Supporting Information). The equatorial positions are occupied by 2,3-methyl-imidazole and pyrazole for complexes IIIa and IIIb, respectively. The computed *D* values are found to be positive in nature for both complexes with a larger *D* value computed for IIIb compared with IIIa. Although the magnitude slightly varies, the computed values are in agreement with the experimental results (see Table 1). The difference in the *D* values observed between IIIa and IIIb arises again due to variation in the structural parameters (see the Supporting Information, Table S2 for details). For both complexes, large negative *D* values arise from excitation I (predominantly $d_{yz} \rightarrow d_{z^2}$ transition) whereas two other excitations (predominantly $d_{xz} \rightarrow d_{z^2}$ and $d_{xy} \rightarrow d_{x^2-y^2}$ transitions) are found to contribute to a positive *D* value as in other groups studied. The excitation analysis reveals significant reduction of the negative contributions to *D* and significant enhancement in the positive *D* contributions for complex IIIb compared with complex IIIa (see Table 2). Here both the $\Delta\alpha$ value (8.3 vs. 0.8 for IIIa and IIIb, respectively) and the $\Delta\beta$ values (2.5 vs. 4.8 for IIIa and IIIb, respectively) are found to differ. The variation of both parameters leads to larger differences for the computed *D* values than for those observed for Group I and II, where only one parameter ($\Delta\alpha$ for Group I and $\Delta\beta$ for Group II) was found to vary. Besides these structural variations, because both the N- and O- donor atoms are present, the donating abilities and the related metal–ligand covalency are also likely to affect the orbital ordering and the computed *D* values.

Studies on Group IV: {$NiN_2O_2O_2'$} complexes

Further diversity is observed with two N-donors, two O-donors, and two O′-donor ligands. The O and O′ atoms represent two different oxygen-donor ligands, namely, water and acetate/formaldehyde groups. All the computed *D* values are found to be positive in nature and this is in contradiction to the experimental observations. Because the experimental values are obtained by fitting the magnetization data, we have also attempted to fit these data with positive *D* values and as expected both positive and negative *D* values are found to fit the experimental data excellently (see Figures S16–S23 in the Supporting Information). Although the sign of *D* is found to vary, the magnitude of the computed *D* value is in agreement with the experiments. More importantly, the experimental trend of IVd < IVb < IVc < IVa is nicely reproduced in our calculations. The nature of the excitations, which contributes to the *D* values, is similar to those of the aforementioned groups. Similar to the Group III, both the $\Delta\alpha$ and the $\Delta\beta$ parameters are found to vary and the variation in these parameters are found to correlate to the magnitude of the computed *D* values (see the Supporting Information, Table S2 and S3 for details).

The role of structural distortions on the estimation of *D* values

To probe how structural distortion can influence the computed *D* values, we decided to take one representative structure (Ib) and developed magneto–structural *D* correlations. Here we have developed two magneto–structural correlations: *cis*-bond elongation[21b] and changes to the $\Delta\beta$ value.

Cis-bond elongation

Because earlier studies emphasis the role of the Ni–L bond lengths, particularly the difference in the Ni–L bond lengths (D_{str}) as a key parameter that controls the sign and magnitude of *D*, herein we decided to develop a magneto–structural correlation by varying the two equatorial *cis*-Ni–N bond lengths. Elongation and compression of this parameter will essentially enhance/decrease the defined D_{str} parameter. Developed magneto–structural correlation for D_{str} versus *D* is shown in Figure 5. As the D_{str} value increases the magnitude of *D* is found to increase, whereas a decrease in the D_{str} value leads to a negative *D* value (note that positive D_{str} values led to positive *D* values, whereas negative D_{str} values led to negative *D* values). A variation of 12 cm^{-1} in the magnitude of *D* (from +4 to −8 cm^{-1}) is observed by altering the D_{str} parameter from −0.3 to 0.55. This illustrates the importance of the bond-length differences in the estimation of the zfs parameter. To gain further insight into the behavior of *D*, we performed orbital analysis and tabulated the major contributory excitations in Table 3. The compression of the equatorial bonds pushes the d orbitals up in energy (see Figure 5). The difference in sign is found to occur due to the trade-off between two excitations: $d_{yz} \rightarrow d_{z^2}$ and $d_{xy} \rightarrow d_{x^2-y^2}$, which are the major contributory transitions in both cases, whereas the third excitation, $d_{xz} \rightarrow d_{z^2}$ remains constant.

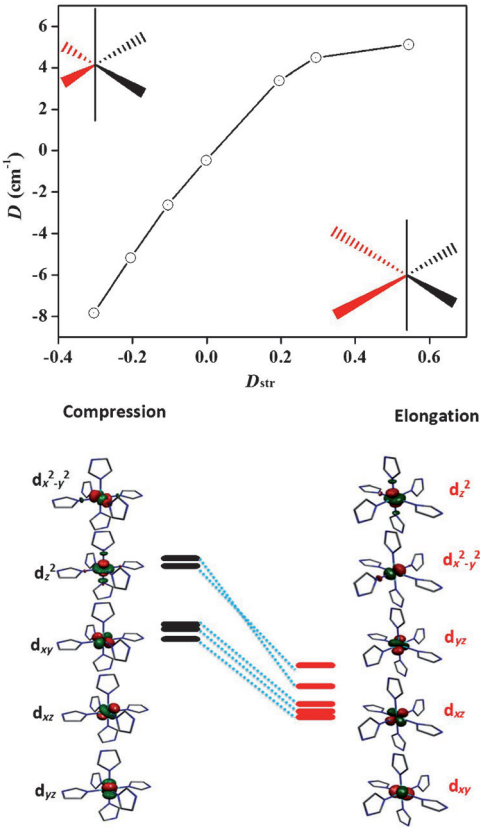

Figure 5. Magneto–structural *D* correlation developed for the D_{str} parameter (top) and computed orbital ordering of the metal-based d orbitals of the Ni^{II} mononuclear complex of Group I upon equatorial compression and elongation (bottom). The red and green regions indicate positive and negative spin phases. The isodensity surface represented corresponds to a value of $0.015e^{-}$ $bohr^{-3}$.

Table 3. CASSCF-computed *D* values for optimized model complexes with different CNs.

CN	Geometry	*D* [cm^{-1}]	*E*/*D*
2	linear	267.51	0.11
3	trigonal	−202.24[a]	0.32
4	tetrahedral	24.69	0.28
5	square pyramidal	25.27	0.06

[a] Since magnitude of *E*/*D* is close to 0.3, sign of *D* parameter is ambiguous.

D correlation for the Δβ parameter

In the second correlation we modified the N_{eq}–Ni–N_{eq} angle to observe the changes in the *D* values. The calculations were performed on the simple homoleptic complex Ib. The parent complex possesses a $\Delta\beta$ value of 1.8 and a $\Delta\alpha$ value of 1.6. To vary the $\Delta\beta$ parameter, the N–Ni–N angle is increased up to 100 degrees and the opposite angle is concurrently reduced to 80 degrees. The variation of $\Delta\beta$ against the computed *D* values is shown in Figure 6. The $d_{xy} \rightarrow d_{x^2-y^2}$ excitation is found to be the major contributing transition and lead to larger positive *D* values as the $\Delta\beta$ increases or decreases. It is apparent from the graph that larger $\Delta\beta$ yield larger *D* values and this is

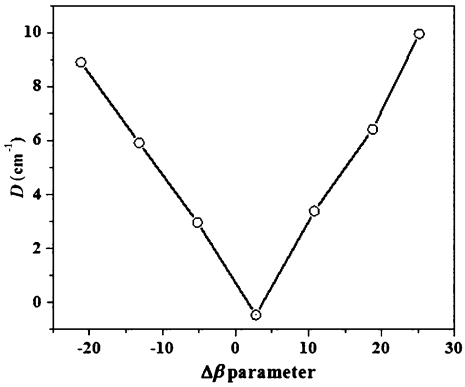

Figure 6. Magneto–structural *D* correlation developed for the $\Delta\beta$ parameter

due to the fact that larger distortions reduce the metal–ligand interaction and in turn decreases the gap between the d_{xy} and $d_{x^2-y^2}$ orbitals, leading to larger *D* values. Note that apart from the $\Delta\beta$ parameter, the $\Delta\alpha$ parameter can also influence the sign and magnitude of the *D* values.

The role of the CN on the computed zfs

In general strong metal–ligand interaction quenches the SOC in transition-metal ions and this in turn significantly reduces the magnetic anisotropy. Because SOC is an important ingredient in the magnetic anisotropy and as it is strongly correlated to the orbital degeneracy, apart from the nontrivial structural distortion, the number of donor ligands can also be tuned to vary the SOC parameter to obtain large *D* values. Inspiration for this work is the work of Long and co-workers who have reported a family of two-coordinate $[Fe(C(SiMe_3)_3)_2]^{-}$ complexes, which are characterized as SMMs and these complexes also possess the largest barrier height reported for magnetization reversal.[9b] A reduction in the CN reduces the metal–ligand repulsion, leading to close-lying d orbitals for low-coordination complexes. In this context, Murugesu and co-workers reported a mononuclear $[Ni(6\text{-}Mes)_2]Br$ (6-Mes = 1,3-bis(2,4,6-trimethylphenyl)-3,4,5,6-tetrahydropyrimidin-2-ylidene) complex where Ni^{I} possesses two coordination and shows slow relaxation of magnetization.[41] Furthermore, in a recent report, Ruiz and co-workers[18b] emphasis that the CN plays a prominent role in controlling the sign/magnitude of *D* values. With this background we attempted to understand the role of the CN in the estimation of *D* values in mononuclear Ni^{II} complexes. We modelled the complex Ia with CN = 2–5 (see Table 3 and Figure 7).

All the structures were optimized with the B3LYP functional and verified as minima by computing the frequencies. Because the structures are fully optimized, these models do not represent the high-symmetry point group of the modelled complexes. On the DFT-computed structures, (see Table S6 in the Supporting Information) regular SA-CASSCF calculations were performed to estimate the *D* and *E* values and the orientation of the *D* tensor (see Table 3 and Figure 7). Our calculations reveal a nice trend where *D* increases with a decrease in CN

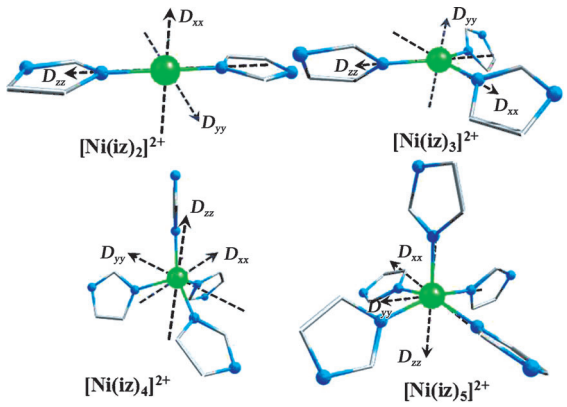

Figure 7. NEVPT2-computed orientation of the *D* tensors for mononuclear two-, three-, four-, and five-coordinated $[Ni(iz)_n]^{2+}$ complex (where $n=2$, 3, 4, and 5).

and a near-linear relationship between *D* and CN is evident. Of particular interest is lower CNs, such as 2 and 3, which yield very large *D* values and illustrate the fact that very large *D* values are achievable by fine tuning the CN.

As calculations on the DFT-optimized model complexes of $[Ni(iz)_n]^{2+}$ generate minimum-energy structures, which are distorted and do not possess the highest-possible symmetry, we decided to extend our studies to $[Ni(NH_3)_n]^{2+}$ models with $n=$ 2–7.[27a]The computed results are summarized in Table 4. This model reiterate the point that lower CN yield large *D* values, but additionally reveals that if the perfect point-group symmetry is maintained, larger *D* values are achievable also with higher CNs, including a trigonal bipyramidal geometry, for which there is experimental evidence of such a large *D* value.[9a] Interestingly, our calculations also predict a large negative *D* for seven-coordinate Ni^{II} complexes and no rhombic zfs parameter for any of the structures. However, all these predictions are yet to be verified by experiments. We have assumed a $S=1$ pseudospin to determine the *D* values, which subsequently quench the orbital momentum.

Table 4. CASSCF + RASSI-SO-computed *D* values for $[Ni(NH_3)_n]^{2+}$ models with $n=2$–7.

CN	Geometry	D_{cal} [cm^{-1}]	E_{cal}	g_{cal} (g_{xx}, g_{yy}, g_{zz})	D_{exp} [cm^{-1}][a]
2	linear	−123.38	0	1.86, 1.86, 2.89	8.6–14.2[42]
3	trigonal planar	96.86	0	1.51, 1.52, 3.80	–
4	square planar	−293.70	0	2.13, 2.11, 1.32	32[43]
4	tetrahedral	−94.54	0	1.89, 1.88, 1.88	55[44]
5	trigonal bipyramidal	−278.27	0	1.43, 1.43, 2.68	−120 to −180[9a]
7	pentagonal bipyramidal	−300.84	0	1.38, 1.38, 1.65	−13.9[27a]

[a] Experimental *D* values reported for relevant structures, but note that none of the reported structures possess the high symmetry defined in the model complexes rendering only tentative cross-comparison.

Conclusion

Magnetic anisotropy is an important ingredient in the design of SMMs. This parameter is extremely difficult to control in polynuclear complexes and till now there is no rational way to enhance the anisotropy for a given SMM. Mononuclear complexes on the other hand, for which the ligand donors, coordination environment, distortion, and CN can be fine tuned, are very versatile. Thus these are attractive building blocks to obtain large anisotropy. Herein we have undertaken detailed ab initio studies on 11 mononuclear Ni^{II} complexes to probe the origin of the magnetic anisotropy and the conclusions derived from this work is summarized below:

1) The studied complexes are divided into four groups according to the type of donor atoms (N or O). The zfs calculations with the NEVPT2-correlated energies yield good numerical estimates of the *D* values in all the cases when compared with the experimental values, albeit the sign of *D* is found to be contrary to experimental values for Group II and IV. More reliable measurements, such as high-field EPR spectroscopy, are required to shed light on the sign of the *D* values.

2) Our magnetic calculations clearly suggest that spin-conserved excitations are the major contributor towards the *D* value. Out of 10 possible spin-conserved excitations, the first three low-lying spin-conserved excitations are the most contributing and play a proactive role in controlling the sign and strength of the *D* values in this class of complexes. However, these excitations are extremely sensitive to structural parameters, such as Ni–L bond lengths and L–Ni–L bond angles. Interestingly, even smaller structural variations are reflected in the computed transition energies and hence found to correlate to the magnitude of the *D* values.

3) The D_{str} parameter, which is correlated to the difference in the Ni–L bond length, is found to significantly influence the sign as well as magnitude of the *D* values. Besides the bond-length parameter, we have defined two more parameters, namely, $\Delta\alpha$ and $\Delta\beta$, which account for the deviation in the *cis* L–Ni–L angles within the coordination environment. These two parameters are also found to significantly influence the strength, but not the sign of the *D* values.

4) The CN is found to be the key parameter to fine tune the zfs parameters as lower CNs are found to yield large *D* values. A near-linear relationship between the CN and the *D* value was detected with *D* as high as $+267\ cm^{-1}$ predicted for two-coordinate mononuclear Ni^{II} complexes. If higher symmetry is maintained, even higher-CN complexes are found to yield very large Ising anisotropy, although this factor is challenging to address experimentally.

Acknowledgements

GR would like to acknowledge financial support from the Government of India through the Department of Science and Technology (SR/S1/IC-41/2010; SR/NM/NS-1119/2011) and Indian Institute of Technology, Bombay to access the high-performance computing facility. S.K.S and T.G. would like to thank CSIR New Delhi and UGC New Delhi, respectively, for SRF fellowships. We also want to thank the anonymous reviewers for their constructive comments.

Keywords: CASSCF calculations · magnetic anisotropy · nickel · magneto–structural correlations · zero-field splitting

[1] a) R. Sessoli, D. Gatteschi, A. Caneschi, M. A. Novak, *Nature* **1993**, *365*, 141 – 143; b) G. Christou, D. Gatteschi, D. N. Hendrickson, R. Sessoli, *MRS Bull.* **2000**, *25*, 66 – 71; c) R. S. D. Gatteschi, J. Villain, *Molecular Nanomagnets*, Oxford University Press, Oxford, **2006**.

[2] a) F. Torres, J. M. Hernandez, X. Bohigas, J. Tejada, *Appl. Phys. Lett.* **2000**, *77*, 3248 – 3250; b) F. Torres, X. Bohigas, J. M. Hernandez, J. Tejada, *J. Phys. Condens. Matter* **2003**, *15*, L119 – L123.

[3] a) M. N. Leuenberger, D. Loss, *Nature* **2001**, *410*, 789 – 793; b) S. Hill, R. S. Edwards, N. Aliaga-Alcalde, G. Christou, *Science* **2003**, *302*, 1015 – 1018; c) F. Troiani, A. Ghirri, M. Affronte, S. Carretta, P. Santini, G. Amoretti, S. Piligkos, G. Timco, R. E. P. Winpenny, *Phys. Rev. Lett.* **2005**, *94*, 207208 – 207204; d) M. Affronte, F. Troiani, A. Ghirri, A. Candini, M. Evangelisti, V. Corradini, S. Carretta, P. Santini, G. Amoretti, F. Tuna, G. Timco, R. E. P. Winpenny, *J. Phys. D* **2007**, *40*, 2999 – 3004; e) A. Ardavan, O. Rival, J. J. L. Morton, S. J. Blundell, A. M. Tyryshkin, G. A. Timco, R. E. P. Winpenny, *Phys. Rev. Lett.* **2007**, *98*, 057201 – 057204; f) R. E. P. Winpenny, *Angew. Chem.* **2008**, *120*, 8112 – 8114; *Angew. Chem. Int. Ed.* **2008**, *47*, 7992 – 7994; g) G. Aromi, D. Aguila, P. Gamez, F. Luis, O. Roubeau, *Chem. Soc. Rev.* **2012**, *41*, 537 – 546; h) J. M. Clemente-Juan, E. Coronado, A. Gaita-Arino, *Chem. Soc. Rev.* **2012**, *41*, 7464 – 7478.

[4] a) O. Waldmann, *Inorg. Chem.* **2007**, *46*, 10035 – 10037; b) F. Neese, D. A. Pantazis, *Faraday Discuss.* **2011**, *148*, 229 – 238.

[5] J. M. Zadrozny, J. Liu, N. A. Piro, C. J. Chang, S. Hill, J. R. Long, *Chem. Commun.* **2012**, *48*, 3927 – 3929.

[6] a) C. J. Milios, M. Manoli, G. Rajaraman, A. Mishra, L. E. Budd, F. White, S. Parsons, W. Wernsdorfer, G. Christou, E. K. Brechin, *Inorg. Chem.* **2006**, *45*, 6782 – 6793; b) C. J. Milios, A. Vinslava, W. Wernsdorfer, S. Moggach, S. Parsons, S. P. Perlepes, G. Christou, E. K. Brechin, *J. Am. Chem. Soc.* **2007**, *129*, 2754 – 2755.

[7] a) N. Ishikawa, M. Sugita, T. Ishikawa, S. Koshihara, Y. Kaizu, *J. Am. Chem. Soc.* **2003**, *125*, 8694 – 8695; b) N. Ishikawa, M. Sugita, T. Ishikawa, S. Koshihara, Y. Kaizu, *J. Phys. Chem. B* **2004**, *108*, 11265 – 11271; c) M. A. Al-Damen, J. M. Clemente-Juan, E. Coronado, C. Marti-Gastaldo, A. Gaita-Arino, *J. Am. Chem. Soc.* **2008**, *130*, 8874 – 8875; d) S. D. Jiang, B. W. Wang, G. Su, Z. M. Wang, S. Gao, *Angew. Chem.* **2010**, *122*, 7610 – 7613; *Angew. Chem. Int. Ed.* **2010**, *49*, 7448 – 7451; e) M. Jeletic, P. H. Lin, J. J. Le Roy, I. Korobkov, S. I. Gorelsky, M. Murugesu, *J. Am. Chem. Soc.* **2011**, *133*, 19286 – 19289.

[8] a) N. Ishikawa, M. Sugita, N. Tanaka, T. Ishikawa, S. Y. Koshihara, Y. Kaizu, *Inorg. Chem.* **2004**, *43*, 5498 – 5500; b) D. E. Freedman, W. H. Harman, T. D. Harris, G. J. Long, C. J. Chang, J. R. Long, *J. Am. Chem. Soc.* **2010**, *132*, 1224 – 1225; c) W. H. Harman, T. D. Harris, D. E. Freedman, H. Fong, A. Chang, J. D. Rinehart, A. Ozarowski, M. T. Sougrati, F. Grandjean, G. J. Long, J. R. Long, C. J. Chang, *J. Am. Chem. Soc.* **2010**, *132*, 18115 – 18126; d) T. Jurca, A. Farghal, P. H. Lin, I. Korobkov, M. Murugesu, D. S. Richeson, *J. Am. Chem. Soc.* **2011**, *133*, 15814 – 15817; e) P. H. Lin, N. C. Smythe, S. I. Gorelsky, S. Maguire, N. J. Henson, I. Korobkov, B. L. Scott, J. C. Gordon, R. T. Baker, M. Murugesu, *J. Am. Chem. Soc.* **2011**, *133*, 15806 – 15809; f) J. M. Zadrozny, J. R. Long, *J. Am. Chem. Soc.* **2011**, *133*, 20732 – 20734.

[9] a) R. Ruamps, R. Maurice, L. Batchelor, M. Boggio-Pasqua, R. Guillot, A. L. Barra, J. Liu, E.-E. Bendeif, S. Pillet, S. Hill, T. Mallah, N. Guihéry, *J. Am. Chem. Soc.* **2013**, *135*, 3017 – 3026; b) J. M. Zadrozny, D. J. Xiao, M. Atanasov, G. J. Long, F. Grandjean, F. Neese, J. R. Long, *Nat. Chem.* **2013**, *5*, 577 – 581.

[10] M. Gruden-Pavlovic, M. Peric, M. Zlatar, P. Garcia-Fernandez, *Chem. Sci.* **2014**, *5*, 1453 – 1462.

[11] A. Solanki, M. Monfort, S. B. Kumar, *J. Mol. Struct.* **2013**, *1050*, 197 – 203.

[12] R. Boča, J. Miklovič, J. TitiŠ, *Inorg. Chem.* **2014**, *53*, 2367 – 2369.

[13] A. Buchholz, A. O. Eseola, W. Plass, *C. R. Chim.* **2012**, *15*, 929 – 936.

[14] a) D.-P. Li, T.-W. Wang, C.-H. Li, D.-S. Liu, Y.-Z. Li, X.-Z. You, *Chem. Commun.* **2010**, *46*, 2929 – 2931; b) Y. L. Wang, Y. Ma, X. Yang, J. K. Tang, P. Cheng, Q. L. Wang, L. C. Li, D. Z. Liao, *Inorg. Chem.* **2013**, *52*, 7380 – 7386; c) S. D. Jiang, S. S. Liu, L. N. Zhou, B. W. Wang, Z. M. Wang, S. Gao, *Inorg. Chem.* **2012**, *51*, 3079 – 3087; d) J. J. Baldoví, S. Cardona-Serra, J. M. Clemente-Juan, E. Coronado, A. Gaita-Arino, A. Palii, *Inorg. Chem.* **2012**, *51*, 12565 – 12574.

[15] K. R. Meihaus, J. R. Long, *J. Am. Chem. Soc.* **2013**, *135*, 17952 – 17957.

[16] a) J. Cirera, E. Ruiz, S. Alvarez, F. Neese, J. Kortus, *Chem. Eur. J.* **2009**, *15*, 4078 – 4087; b) R. Boča, *Coord. Chem. Rev.* **2004**, *248*, 757 – 815; c) R. Maurice, C. de Graaf, N. Guihery, *J. Chem. Phys.* **2010**, *133*, 084307 – 084312.

[17] a) F. Neese, *J. Am. Chem. Soc.* **2006**, *128*, 10213 – 10222; b) F. Neese, T. Petrenko, D. Ganyushin, G. Olbrich, *Coord. Chem. Rev.* **2007**, *251*, 288 – 327; c) S. Zein, C. Duboc, W. Lubitz, F. Neese, *Inorg. Chem.* **2008**, *47*, 134 – 142; d) C. Duboc, D. Ganyushin, K. Sivalingam, M. N. Collomb, F. Neese, *J. Phys. Chem. A* **2010**, *114*, 10750 – 10758; e) D. Maganas, S. Sottini, P. Kyritsis, E. J. J. Groenen, F. Neese, *Inorg. Chem.* **2011**, *50*, 8741 – 8754.

[18] a) E. Cremades, E. Ruiz, *Inorg. Chem.* **2011**, *50*, 4016 – 4020; b) S. Gomez-Coca, E. Cremades, N. Aliaga-Alcalde, E. Ruiz, *J. Am. Chem. Soc.* **2013**, *135*, 7010 – 7018.

[19] a) C. Cadiou, M. Murrie, C. Paulsen, V. Villar, W. Wernsdorfer, R. E. P. Winpenny, *Chem. Commun.* **2001**, 2666 – 2667; b) E. C. Yang, W. Wernsdorfer, S. Hill, R. S. Edwards, M. Nakano, S. Maccagnano, L. N. Zakharov, A. L. Rheingold, G. Christou, D. N. Hendrickson, *Polyhedron* **2003**, *22*, 1727 – 1733; c) J. Lawrence, E. C. Yang, R. Edwards, M. M. Olmstead, C. Ramsey, N. S. Dalal, P. K. Gantzel, S. Hill, D. N. Hendrickson, *Inorg. Chem.* **2008**, *47*, 1965 – 1974.

[20] a) M. Atanasov, P. Comba, S. Helmle, D. Muller, F. Neese, *Inorg. Chem.* **2012**, *51*, 12324 – 12335; b) S. F. Ye, F. Neese, *J. Chem. Theory Comput.* **2012**, *8*, 2344 – 2351.

[21] a) R. Maurice, R. Bastardis, C. de Graaf, N. Suaud, T. Mallah, N. Guihery, *J. Chem. Theory Comput.* **2009**, *5*, 2977 – 2984; b) R. Maurice, L. Vendier, J. P. Costes, *Inorg. Chem.* **2011**, *50*, 11075 – 11081; c) R. Maurice, C. de Graaf, N. Guihery, *Phys. Chem. Chem. Phys.* **2013**, *15*, 18784 – 18804.

[22] a) J. N. Rebilly, G. Charron, E. Riviere, R. Guillot, A. L. Barra, M. D. Serrano, J. van Slageren, T. Mallah, *Chem. Eur. J.* **2008**, *14*, 1169 – 1177; b) G. Charron, F. Bellot, F. Cisnetti, G. Pelosi, J. N. Rebilly, E. Riviere, A. L. Barra, T. Mallah, C. Policar, *Chem. Eur. J.* **2007**, *13*, 2774 – 2782; c) G. Rogez, J. N. Rebilly, A. L. Barra, L. Sorace, G. Blondin, N. Kirchner, M. Duran, J. van Slageren, S. Parsons, L. Ricard, A. Marvilliers, T. Mallah, *Angew. Chem.* **2005**, *117*, 1910 – 1913; *Angew. Chem. Int. Ed.* **2005**, *44*, 1876 – 1879.

[23] A. Abragam, B. Bleaney, *Electron Paramagnetic Resonance of Transition Ions*, Dover Publications, Dover, New York, **1986**.

[24] M. Atanasov, P. Comba, C. A. Daul, *Inorg. Chem.* **2008**, *47*, 2449 – 2463.

[25] a) D. Collison, M. Murrie, V. S. Oganesyan, S. Piligkos, N. R. J. Poolton, G. Rajaraman, G. M. Smith, A. J. Thomson, G. A. Timko, W. Wernsdorfer, R. E. P. Winpenny, E. J. L. McInnes, *Inorg. Chem.* **2003**, *42*, 5293 – 5303; b) S. Piligkos, E. Bill, D. Collison, E. J. L. McInnes, G. A. Timco, H. Weihe, R. E. P. Winpenny, F. Neese, *J. Am. Chem. Soc.* **2007**, *129*, 760 – 761; c) S. Piligkos, H. Weihe, E. Bill, F. Neese, H. El Mkami, G. M. Smith, D. Collison, G. Rajaraman, G. A. Timco, R. E. P. Winpenny, E. J. L. McInnes, *Chem. Eur. J.* **2009**, *15*, 3152 – 3167.

[26] A. Kubica, J. Kowalewski, D. Kruk, M. Odelius, *J. Chem. Phys.* **2013**, *138*, 064304 – 064309.

[27] a) R. Ruamps, L. J. Batchelor, R. Maurice, N. Gogoi, P. Jiménez-Lozano, N. Guihéry, C. de Graaf, A.-L. Barra, J.-P. Sutter, T. Mallah, *Chem. Eur. J.* **2013**, *19*, 950 – 956; b) J.-P. Costes, R. Maurice, L. Vendier, *Chem. Eur. J.* **2012**, *18*, 4031 – 4040.

[28] J. Titis, R. Boca, *Inorg. Chem.* **2010**, *49*, 3971 – 3973.

[29] R. Boca, J. Titis, in *Coordination Chemistry Research Progress* (Eds.: T. W. Cartere, K. S. Verley), NOVA Publishers, **2008**, pp. 247 – 304.

[30] F. Neese, *WIREs Comput. Mol. Sci.* **2012**, *2*, 73 – 78.

[31] a) P. Baran, M. Boca, R. Boca, A. Krutosikova, J. Miklovic, J. Pelikan, J. Titis, *Polyhedron* **2005**, *24*, 1510 – 1516; b) R. Ivanikova, R. Boca, L. Dlhan, H. Fuess, A. Maslejova, V. Mrazova, I. Svoboda, J. Titis, *Polyhedron* **2006**, *25*, 3261 – 3268; c) A. Maslejova, R. Ivanikova, I. Svoboda, B. Papankova, L. Dlhan, D. Miklos, H. Fuess, R. Boca, *Polyhedron* **2006**, *25*, 1823 – 1830; d) J. Titis, R. Boca, L. Dlhan, T. Durcekova, H. Fuess, R. Ivanikova, V. Mrazova, I. Svoboda, *Polyhedron* **2007**, *26*, 1523 – 1530.

[32] F. Neese, E. I. Solomon, *Inorg. Chem.* **1998**, *37*, 6568 – 6582.

[33] M. R. Pederson, S. N. Khanna, *Phys. Rev. B* **1999**, *60*, 9566 – 9572.

[34] F. Weigend, R. Ahlrichs, *Phys. Chem. Chem. Phys.* **2005**, *7*, 3297 – 3305.

[35] D. Ganyushin, F. Neese, *J. Chem. Phys.* **2006**, *125*, 024103 – 024111.

[36] a) C. Angeli, R. Cimiraglia, S. Evangelisti, T. Leininger, J. P. Malrieu, *J. Chem. Phys.* **2001**, *114*, 10252 – 10264; b) C. Angeli, R. Cimiraglia, J. P. Malrieu, *Chem. Phys. Lett.* **2001**, *350*, 297 – 305; c) C. Angeli, R. Cimiraglia, J. P. Malrieu, *J. Chem. Phys.* **2002**, *117*, 9138 – 9153.

[37] a) F. Aquilante, L. De Vico, N. Ferre, G. Ghigo, P. A. Malmqvist, P. Neogrady, T. B. Pedersen, M. Pitonak, M. Reiher, B. O. Roos, L. Serrano-Andres, M. Urban, V. Veryazov, R. Lindh, *J. Comput. Chem.* **2010**, *31*, 224 – 247; b) L. F. Chibotaru, L. Ungur, *J. Chem. Phys.* **2012**, *137*, 064112 – 064122; c) J. A. Duncan, *J. Am. Chem. Soc.* **2009**, *131*, 2416 – 2416; d) G. Karlström, R. Lindh, P. A. Malmqvist, B. O. Roos, U. Ryde, V. Veryazov, P. O. Widmark, M. Cossi, B. Schimmelpfennig, P. Neogrady, L. Seijo, *Comput. Mater. Sci.* **2003**, *28*, 222 – 239; e) V. Veryazov, P. O. Widmark, L. Serrano-Andres, R. Lindh, B. O. Roos, *Int. J. Quantum Chem.* **2004**, *100*, 626 – 635.

[38] P. A. Malmqvist, B. O. Roos, B. Schimmelpfennig, *Chem. Phys. Lett.* **2002**, *357*, 230 – 240.

[39] N. F. Chilton, R. P. Anderson, L. D. Turner, A. Soncini, K. S. Murray, *J. Comput. Chem.* **2013**, *34*, 1164 – 1175.

[40] A. Bencini, D. Gatteschi, *Electron Paramagnetic Resonance of Exchange Coupled Systems*, Springer, **2011**.

[41] R. C. Poulten, M. J. Page, A. G. Algarra, J. J. Le Roy, I. Lopez, E. Carter, A. Llobet, S. A. Macgregor, M. F. Mahon, D. M. Murphy, M. Murugesu, M. K. Whittlesey, *J. Am. Chem. Soc.* **2013**, *135*, 13640 – 13643.

[42] P. Mukherjee, M. G. B. Drew, V. Tangoulis, M. Estrader, C. Diaz, A. Ghosh, *Polyhedron* **2009**, *28*, 2989 – 2996.

[43] K. Ray, A. Begum, T. Weyhermüller, S. Piligkos, J. van Slageren, F. Neese, K. Wieghardt, *J. Am. Chem. Soc.* **2005**, *127*, 4403 – 4415.

[44] D. Maganas, A. Grigoropoulos, S. S. Staniland, S. D. Chatziefthimiou, A. Harrison, N. Robertson, P. Kyritsis, F. Neese, *Inorg. Chem.* **2010**, *49*, 5079 – 5093.

Received: March 20, 2014
Published online on July 17, 2014